Model Tests on Screening of Surface Waves

Expériments en Echelle Reduite sur l'Isolation des Ondes de Surface

W.A. HAUPT Project Engineer, Landesgewerbeanstalt Bayern, Nürnberg, Fed. Rep. of Germany

SYNOPSIS Tests in model scale have been performed on the vibration isolation effect of various measures in the ground. Solid barriers like concrete core walls as well as rows of bore holes and open trenches are considered. The results are compared to those of theoretical investigations. Emphasis is layed on practical problems in test performance.

INTRODUCTION

A wave source at the ground surface - for instance a vibrating machine foundation - generates both body waves (P- and S-wave) which radiate into the inner of the half-space and mainly the so-called Rayleigh wave (R-wave). This wave type is coupled to the free surface and it transmits the major part of the dynamic energy emitted into the ground (Miller and Pursey, 1954). Therefore and due to the higher geometrical damping of the body waves the wave-field at a distance of more than about one R-wave length from the vibrating foundation, and near to the surface, is determined almost by this Rayleigh wave alone. Hence, it is called Rayleigh wave-field or far-field, whereas the region of body wave dominance close to the wave source is referred to as near-field.If a building or any shock-sensitive installation in the far-field has to be isolated from ground vibrations it is necessary mainly to reduce the R-wave amplitudes by appropriate measures which are located near to the surface.

This paper deals with experimental investigations on various isolation measures. Tests in model scale have been performed to study the screening effect of solid barriers like concrete core walls and of rows of bore holes. In addition open trenches have been considered (Gudehus and Haupt, 1978).

PRIOR INVESTIGATIONS

Experimental investigations in model scale on open trenches have been performed by Woods (1968). He observed an average amplitude reduction of the vertical surface wave component in the far-field down to 25 % at a trench depth of about 1.2 to 1.5 λ_z (λ_z = wave length of surface wave). The same screening effect was obtained in the near-field at trench depths of about 0.6 λ_z. Dolling (1971) conducted measurements on the screening effect of plane slurry filled trenches having a maximum depth of 6 m. The results of calculations by Finite Element method (FE) performed by Segol et al. (1978)

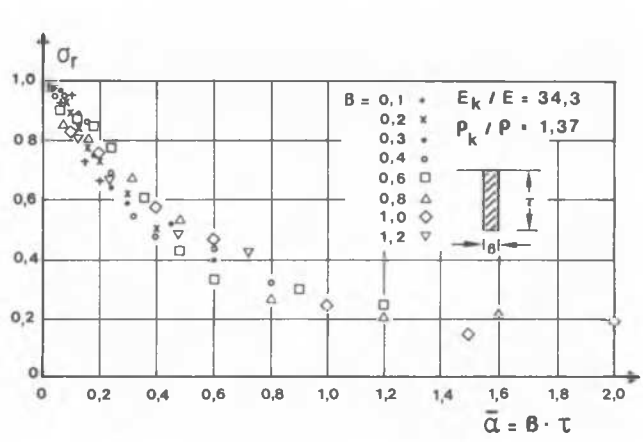

Fig. 1 : Ampl. reduction factor vs $\bar{\alpha}$ from FE-calculations (stiff material obstacles)

are essentially in agreement with the experimental ones. Woods and cooperators reported on first tests on rows of bore holes as isolating measures using the holographic interferometry-technique (Woods, Barnett and Sagesser, 1974).

A large quantity of FE-calculations on the screening effect of plane solid wave barriers like concrete core walls or concrete slabs at the surface have been performed by Haupt (1978 a, 1978 b). By use of the influence matrix procedure (Haupt, 1978 c) the plane wave-field in the vicinity of these solid obstacles could be studied and the physical reason of their isolation effect be explained. Varied parameters have been the cross sectional shape, the dimensions, the material properties and the distance to the wave source. The screening effectiveness has been expressed by the amplitude reduction factor, σ_r, which gives the average reduction of the vertical vibration component at the surface caused by the barrier behind it.

One of the most interesting results of this study on rigid obstacles (concrete) is the relationship between σ_r and the normalized cross sectional area $\bar{a}$, see Fig. 1. In this figure β and τ are the dimensions of the cross section normalized on λ_z and $\bar{a}$ equals $\beta \cdot \tau$.

From this figure it is to be stated that σ_r does not depend on the actual cross sectional shape of the obstacle but only on the normalized cross sectional area $\bar{a}$.

TEST FACILITIES

The measurements were performed in a sand bin with dimensions of 9.6 x 9.7 m and a depth of about 3 m located in the test hall of the Institute of Soil and Rock Mechanics, University of Karlsruhe, see Fig. 2. The soil in the bin consisted of a medium to coarse sand. To achieve as much homogeneity as possible the sand was placed at its highest possible density by compacting layers of 30 cm thickness by passing 10 times crosswise. It has been found from preliminary tests that more passes did not result in a better compaction.

The density of the sand was controlled at each layer yielding an almost constant value of $\rho = 1.72$ t/m^3, which corresponds to a void ratio of $e = 0.56$ at a water content of 3 %.

The soil surface inside the bin was paved letting open a center circular area of 4 m radius, where the measurements were conducted. Access to this measurement area was possible by a bridge reaching from the pavement to a column, which was fixed at the ceiling of the hall above the center of the free area. Using this arrangement the bridge could be twisted horizontally around this center point. Furthermore, it was shifted to the side in a way, that measurements could be performed along a radius of the circular area, see Fig. 2 b.

In the center of the circular area an electrodynamic vibrator of 40 W power was located at the surface generating a concentric, steady-state harmonic wave-field. The vertical component of this wave-field at the surface was measured by placing a vibration transducer along a radius at constant intervals of 5 cm or 2.5 cm at small wave-lengths respectively. Very light weight (0.3 N) accelerometers were used as transducers. For the schematic of instrumentation see Fig. 3.

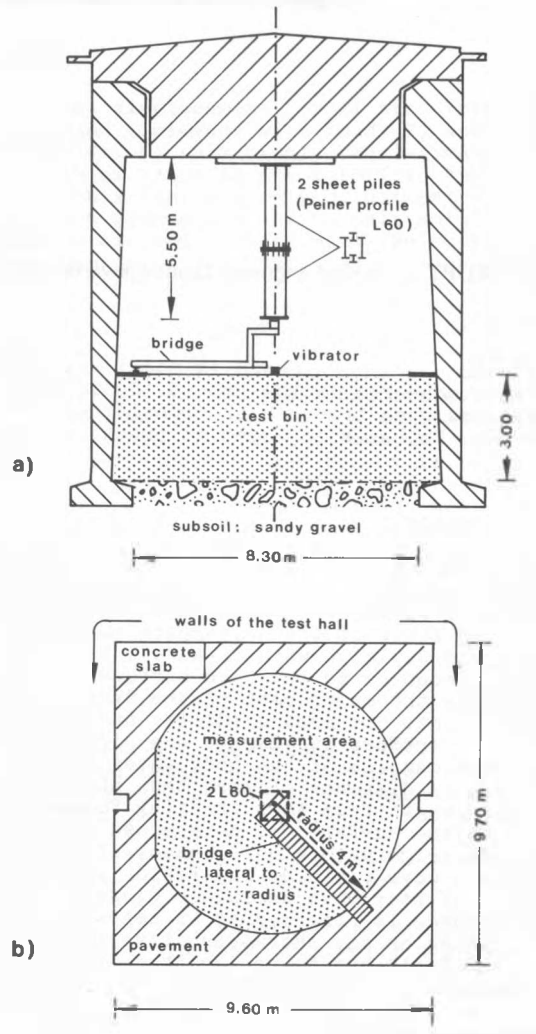

Fig. 2 : Test facility
a) Cross section of the test hall
b) Plane view of the sand bin

At each point the amplitude of the vibration and the phase angle with respect to a reference vibration were measured. For this purpose a second transducer was placed on the vibrator, yielding a reference signal which was observed at the screen of an oscilloscope. The phase shift between the signal of the transducer on the sand and the reference signal could then be read from the screen with an accuracy of less than 1 % of one period. The inverse slope of the phase angle curve with distance represents the wave length.

An important problem in performing the measurements was the coupling of the transducer to the ground. On one hand it had to be heavy enough to assure good contact to the soil when being slowly set down on the sand, on the other hand the weight had to be small enough not to cause traces at the surface since several measurements were performed at one point during each test. Furthermore, the natural frequency f_n of the transducer on the ground should not have been near the generated wave frequency f_a, because in case of resonance small changes in the coupling conditions resulted in large differences of the measured amplitudes.

The final shape of the transducer-plate (see Fig. 4) found from preliminary tests consisted of a steel plate with various dimensions and a PVC contact disc of 20 mm diameter. The

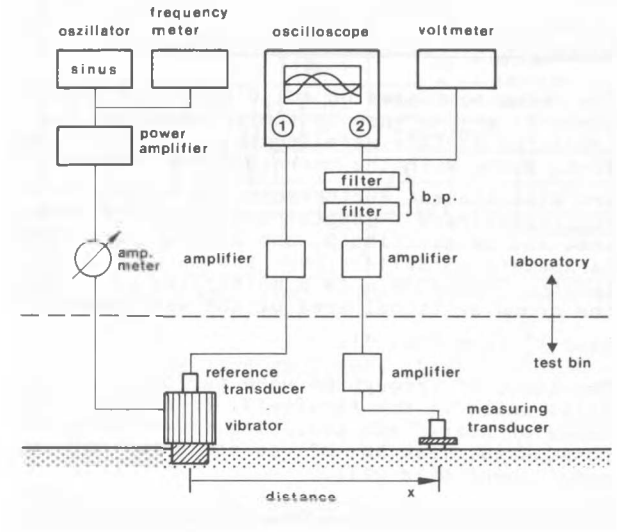

Fig. 3 : Schematic of instrumentation

properties were as follows:

$f_a \leq 320$ Hz: G = 3.6 N
$f_n \approx 200$ Hz, D $\approx$ 0.04

$f_a > 320$ Hz: F = 2.5 N
$f_n \approx 239$ Hz, D $\approx$ 0.055

where G is the weight and D the damping ratio. The natural frequency and the damping were measured by plucking the transducer in vertical direction and observing the decay curve of the free vibration. The difference between f_a and f_n turned out to be large enough for practical purposes: the amplitudes of the vibrations at repeated measurements under the same conditions varied of at maximum 9 % and the phase angle of 1 to 2 %.

A further difficulty consisted in the water content of the sand variing with time. To avoid drying of the soil the surface was covered by a plastic sheet of 0.5 mm thickness. It had to be removed during the performance of the measurements which resulted in small changes of the water content of the sand close to the surface. Although there was no influence on the propagation characteristics of the waves to be observed the coupling conditions were affected considerably. This source of error could be avoided by using a second plastic sheet of 0.03 mm thickness resting at place during the measurements.

Close to the walls of the sand bin some reflection of the incoming waves could be observed. It was tried to reduce this effect by placing plates of rubber foam tangentially around the measurement area. The cross sectional shape and the angle of inclination of these plates were chosen to transmit at maximum the energy of an incoming shear wave but to reflect those waves which were travelling back from the

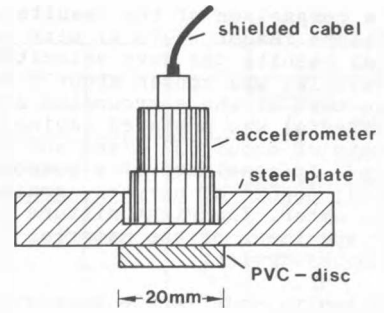

Fig. 4 : Transducer plate

concrete walls.

However, by this measure no reduction of the amplitudes of the reflected waves was achieved, on the contrary the reflections were even increased. Therefore the plates have been removed again.

Since the wave velocity depends on the state of stress in the soil it usually varies with depth. At the measurements, therefore, the surface wave will not be exactly the theoretical Rayleigh wave. Hence, it will be referred to as R_z-wave (wave length λ_z) in the following.

TEST PERFORMANCE

The investigations were performed by first measuring the wave field along a radius at a given frequency without any obstacle, after that placing the obstacle and then measuring again. The solid walls and the rows of bore holes were plane and oriented perpendicular to the direction of propagation of the waves. The distance to the vibrator (x_0) was between 1.65 and 1.8 m and their length to each side of the radius about 0.5 to 0.6 m. The solid walls had rectangular cross sectional shape, reaching from the surface into the ground. They were prefabricated and placed by digging a trench at the position of the wall, inserting them and carefully refilling the remaining gap. The value of λ_z was usually chosen to be about 24, 30 and 40 cm, which correspondend to frequencies between about 380 Hz and 240 Hz. In some cases (at bore holes) wave lengths of about 18 cm (590 Hz) and of 50 cm (224 Hz) were used. Hence, the wave barriers were by far located in the far-field. In addition some special tests on near-field isolation measures were conducted.

The profile of the shear wave velocity with depth as obtained from R_z-wave dispersion measurements and from cross-hole tests is presented in Fig. 5. The wave velocity in the soil varied to some amount with time due to changes in water content, which caused variations of the apparent cohesion. Therefore, prior to each test measurements of the wave velocity were conducted, which served to calculate the frequencies yielding the desired wave lengths.

To enable a comparison of the results of the FE-calculations (Haupt, 1978 a) with the experimental results the wave velocity of the obstacle material was chosen about 5 times higher than that of the surrounding sand. Hence, a material was prepared having a shear wave velocity of about 530 m/sec and a density of 2.32 t/m^3. It consisted of a compound of gypsum, sand, powder of barytes, grains of barytes and water. The right mixture was found by testing specimens of the material in the resonant-column-device.

The bore holes in model scale were supported by plastic tubes. The material RNF 100 was found to be the most suitable because it was soft but still stiff enough so that the tubes could be installed. For producing a bore hole this tube was pushed over a metal pipe which was guided to move in vertical direction. With the tubes penetrating into the ground, the sand was sucked through the pipe by vacuum. Due to frictional effects the maximum depth obtainable by this procedure was about 30 cm. The minimum spacing of the holes without openings between them was 8 mm.

All measurements have been performed two times and the average value was used for the further analysis. This was done by calculating the normalized amplitude

$$\gamma_v(x) = \frac{U(x)}{U_z(x)}$$

where U(x) represents the amplitude of the vertical component depending on the distance x in the case of an obstacle within the wave field and U_z (x) is the amplitude of the undisturbed R_z-wave field. The screening effect of the obstacles is expressed by the amplitude reduction factor, σ_r, which is the average value of γ_v (x) behind the obstacle:

$$\sigma_r = \frac{1}{x_2 - x_1} \cdot \int_{x_1}^{x_2} \gamma_v(x)\, dx \quad .$$

The considered interval reaches from immediately behind the obstacle (x_1) to x_2, where this is not a constant value because reflections from the walls of the test bin in some cases influenced the amplitude, see Fig. 7.

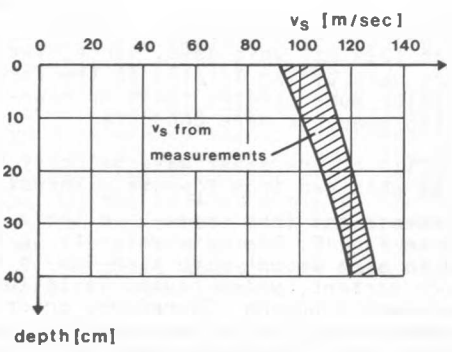

Fig. 5 : Shear wave velocity profile with depth

TEST RESULTS

Screening effect of solid obstacles

The tests conducted on solid obstacles (see Table I) are defined by their number and the projected surface wave length. The actual values of λ_z along with the corresponding frequency f_a are also listed. Furthermore the dimensions B (thickness) and T (depth) are given for each test and in addition β and τ, which are these parameters normalized over the surface wave length. The value $\bar{a}$ is β multiplied by τ, e.g. the cross sectional area of the wall normalized over λ_z^2 (see Fig. 1).

The tests M1 through M6 were performed with solid walls in the far-field. In addition two cases of near-field isolation (M2/N, M5/N) were considered. Test No. M7 was concerned with a model sheet pile wall.

In Fig. 6 and 7 the normalized amplitudes $\gamma_v(x)$ obtained at a thin, deep wall (M2/30) and a wide, shallow one (M4/30) are presented as examples. Also in these figures are plotted the corresponding curves from the FE-calculations performed at obstacles with the same normalized dimensions.

In front of the barriers a distinct interference pattern can be observed in both cases. Here the curves from the calculations and the measurements coincide very well concerning the location of the peaks as well as the attenuation of the peak values with increasing distance from the wall. The horizontal spacing between two peaks is almost exactly $\lambda_z/2$, which indicates the incoming Rayleigh wave being partly reflected at the walls.

Behind the obstacles a substantial reduction of the amplitudes can be observed in both the measured and the calculated cases. The measured curves show considerable variations. However, if the mean value is considered the curves from the experiments are in good agreement with the calculated one.

Fig. 8 shows the case of a near-field isolation where the same wall is used as in test No M2/30. Comparing Fig. 6 and Fig. 8 it can be stated, that the isolation in the near field is obviously more effective than in the far-field. This result is in full agreement with those of the theoretical investigations. Furthermore, at the measurement the amplitude reduction seems to be even greater than at the calculation. This in fact is to be expected because the near field isolation test as performed in this investigation is a threedimensional problem (plane wall in concentric wave field), whereas the FE-calculations are dealing only with the two-dimensional case.

In Fig. 9 σ_r and $\bar{a}$ are presented in the same way as in Fig. 1, e.g. the amplitude reduction factor is plotted versus $\bar{a}$. The narrow band which had been obtained for σ_r from the calculations on solid obstacles in the far-field is indicated

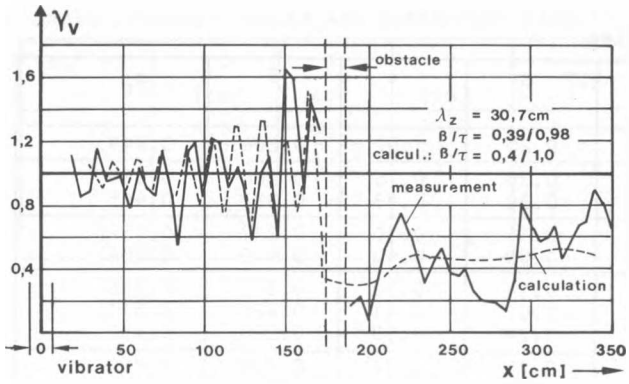

Fig. 6: Normalized amplitude, test No M2/30

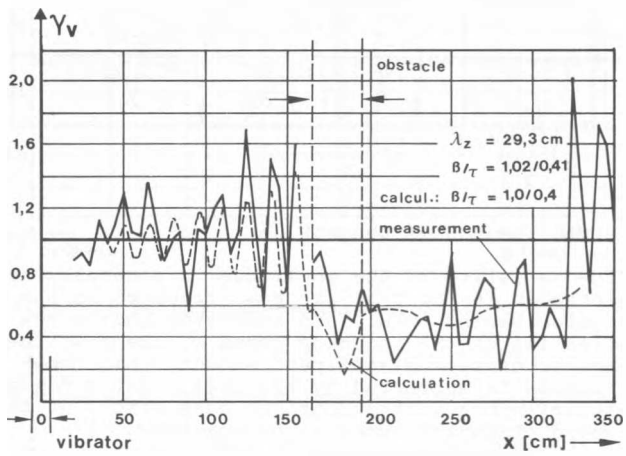

Fig. 7: Normalized amplitude, test No M4/30

by the two dashed curves. As can be seen, most of the σ_r-values from the experiments are located within this narrow band. The smaller values of M5/30 and M5/24 can be explained by the fact, that the obstacle wall had dried out since several weeks before running the test and therefore the material showed a shear wave velocity of about 800 m/sec. However, corresponding FE-calculations with high-velocity material have confirmed these results (Haupt, 1978 a). The triangles in Fig. 9 indicate the results of the near-field isolation tests.

The agreement between the test results and those of the FE-calculations has proven the reliability of the theoretical results. Hence, the finding of the FE-study has been confirmed: The screening effect of solid obstacles in the ground does not depend on their actual shape, but only on their normalized cross sectional area. Furthermore, near-field isolation was found to be more effective than far-field isolation.

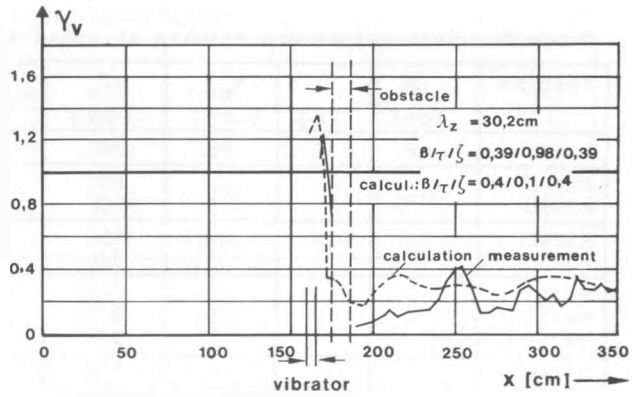

Fig. 8: Normalized amplitude, test No M2/N ($\zeta = x_0/\lambda_z$)

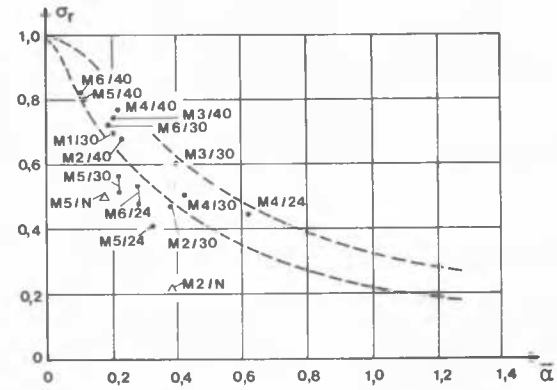

Fig. 9 : σ_r vs $\bar{\alpha}$ from tests on solid obstacles

Sheet pile walls

Sheet pile walls are sometimes considered as effective vibration isolation measures. Therefore the test No. M7 was performed using a model sheet pile wall of 30 cm depth, a length of 120 cm and dimensions of the profile as shown in Fig. 10

From Table I it can be seen that the screening effect of this type of obstacle is not satisfactory at least for values of its depth which are in the order of the wave-length. Woods (1968) has also pointed to this fact. However, higher effectiveness might be expected at smaller wave-lengths.

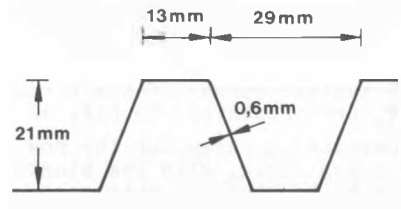

Fig. 10: Dimensions of model sheet pile wall

Table I : Test values and results at solid obstacles

Test No	B [cm]	T [m]	x_o [cm]	f_a [Hz]	λ_z [cm]	β	τ	$\bar{\alpha}$	σ_r
M1/30	6	30	165	320	29.7	0.20	1.02	0.204	0.699
M2/40	12	30	175	260	39.7	0.30	0.76	0.288	0.680
M2/30				320	30.7	0.39	0.98	0.382	0.465
M3/40	30	12	175	253	40.7	0.74	0.30	0.217	0.752
M3/30				326	30.0	1.00	0.40	0.400	0.604
M4/40	30	12	165	240	40.6	0.74	0.30	0.219	0.756
M4/30				320	29.3	1.02	0.41	0.425	0.511
M4/24				385	24.1	1.24	0.50	0.620	0.452
M5/40	6	30	177	270	39.0	0.15	0.77	0.118	0.800
M5/30				340	29.1	0.21	1.03	0.213	0.414/0.456
M5/24				404	23.4	0.26	1.28	0.329	0.410
M6/40	30	6	170	264	40.0	0.75	0.15	0.113	0.817
M6/30				328	30.4	0.99	0.20	0.195	0.725
M6/24				379	25.5	1.18	0.24	0.277	0.480/0.530
M7/40		30	180	258	39.4		0.76		0.952
M7/30				322	29.6		1.01		0.783
M7/24				385	23.6		1.27		0.849
M2/N	12	30	12	320	30.7	0.39	0.98	0.382	0.215
M5/N	6	30	12	320	30.6	0.20	0.98	0.192	0.494

Screening effect of rows of bore holes

Possible geometrical parameters of influence on the isolation effect of rows of bore holes are the diamter D, the spacing E and the depth T. These parameters normalized over λ_z are referred to as δ, ε and τ. The dimensionless cross sectional area as used in the case of solid walls is considered not to be a meaningful parameter at rows of bore holes. Instead of this the relativ normalized shielded area $\bar{\beta}$ was defined, which is

$$\bar{\beta} = \frac{\delta}{(\delta+\varepsilon)} \quad \tau = \frac{D}{(D+E)} \frac{T}{\lambda_z}$$

Because of the dimensionless depth τ this parameter depends on the wave length, whereas the expression $\delta/(\delta+\varepsilon)$ represents a purely geometrical parameter of the row.

A total number of 6 test series has been performed varying mainly the diameter and the spacing of the bore holes, see Table II. At each test series several wave lengths ranging from about 18 cm to 50 cm have been used. In Table II also the normalized shielded area $\bar{\beta}$ and the amplitude reduction factor for rows of bore holes, σ_r^r, are included. Due to difficulties in producing the bore holes not all tests could be considered in the analysis (B1, B3).

The calculation of the amplitude reduction factor in this case is based on an interval ranging from the row to constantly x_2 = 370 cm.

In Fig. 11 and 12 typical curves of the normalized amplitude γ_v are presented. In Fig. 12 in addition the corresponding curve for the row of unsupported bore holes - e.g. with the plastic tubes removed - is to be seen. In this case this results in a considerable increase of the effectiveness of the row.

The variation of the amplitude is generally not inhanced in front of the rows compared to the region behind them. This indicates that a reflection of the incoming waves at the rows does not occur to a significant amount. This conclusion is supported by the fact, that a regular interference pattern, as has been stated at the solid obstacles, can not be observed.

From the published results of investigations (Woods, 1974) the parameter ε had been expected to influence the effectiveness of the rows. It has been found, however, that σ_r^r does not show a strong and systematic dependency on ε and has rather to be considered as independent of this parameter. Furthermore, a significant correlation between $\sigma/(\delta+\varepsilon)$ and σ_r^r could not be stated. Only if additionally the normalized depth is considered by relating σ_r^r to $\bar{\beta}$ a significant functional connection is found, see Fig. 13.

The reason for the described relationship is regarded to be the stiffness of the plastic tubes. Part of the energy of the waves it transmitted by this relatively stiff material across the row of bore holes, thus reducing the isolation effect. If the spacing between the holes is decreased, which can be expected to be accompagnied by a greater effectiveness of the row, more stiff tube material exists in the row, by which the effect again is reduced. The influence of the tube stiffness may also be recognized by the relationship between σ_r^r and τ which essentially is represented in Fig. 13 and which is typical for thin and deep, stiff obstacles.

It has been tried to remove the tubes off the holes after the tests to perform measurements at unsupported holes. A result of such a test is

Table II: Test values and summarized results at rows of bore holes

Test No	D [cm]	E [cm]	T [cm]	$\frac{\delta}{\delta+\varepsilon}$	λ_z [cm] from	λ_z [cm] to	$\bar{\beta}$ from	$\bar{\beta}$ to	σ_r^r from	σ_r^r to
B2	1,35	0,8	20,0	0,63	17,7	31,7	0,40	0,71	0,79	0,89
B4	2,75	2,75	28,0	0,5	21,5	39,6	0,36	0,65	0,76	0,87
B5	2,75	2,20	28,0	0,56	21,7	38,0	0,41	0,72	0,71	0,95
B6	2,75	1,65	28,0	0,625	21,2	50,0	0,35	0,83	0,67	0,94
B7	2,75	1,10	28,0	0,714	22,0	50,5	0,40	0,91	0,64	0,84
B8	1,35	0,8	15,0/21,0	0,628	20,9	49,7	0,19	0,87	0,83	1,14

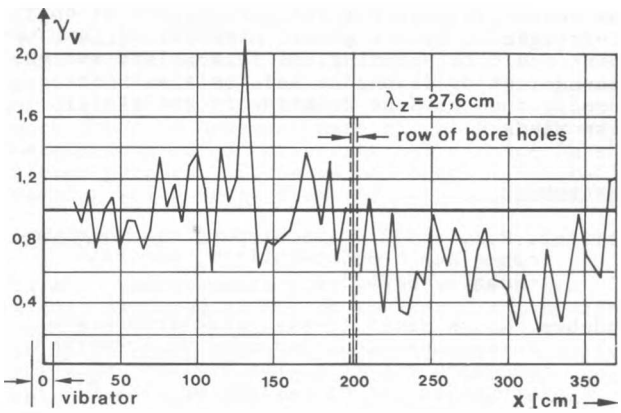

Fig. 11: Normalized amplitude, test No B7

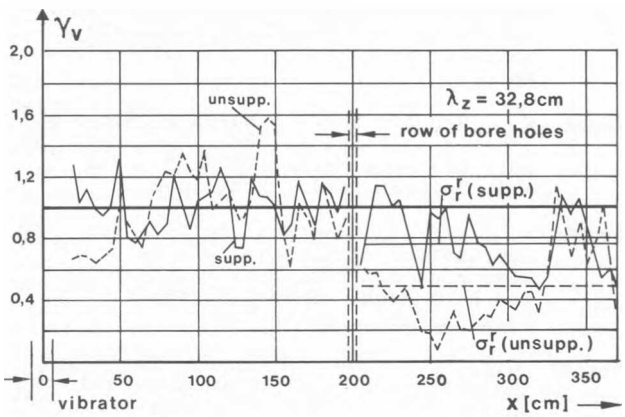

Fig. 12: Normalized amplitude, test No B6

presented in Fig. 12 where a decrease of σ_r^r can be stated. However, it was very difficult to produce rows of unsupported holes in this way without creating interconnections between them. Therefore, only few tests of this type could be performed, from which a systematic relationship could not be deduced. Further investigations on the influence of the bore hole support are desirable because of its significance for practical isolation problems.

Screening effect of open trenches

In connection with the presently described tests also measurements at open trenches had been performed. A typical curve of γ_v (x) is presented in Fig. 14. In front of the trench a distinct and relatively regular interference pattern can be observed which indicates the reflection of most of the wave energy. Behind the trench usually two regions may be distinguished: close to the trench the amplitudes are very low. At some distance, however, the amplitudes increase again yielding a higher amplitude reduction factor for the total region behind the trench. This phenomenon is considered to be caused by waves refracted at the ends of the trench. The refraction angle was found to be about 45° with a tendency to greater angles at smaller wave lengths.

The amplitude reduction factor, σ_r^s depending on τ is plotted in Fig. 15. The open circles are valid for the region close to the trench, whereas the solid circles represent the average value behind the trench. Also given are the results by Woods (1968).

The dashed curve represents σ_r^s from Dolling's (1970) theory. He assumed the energy, which is included in that part of the Rayleigh wave ranging from the surface to the bottom of the

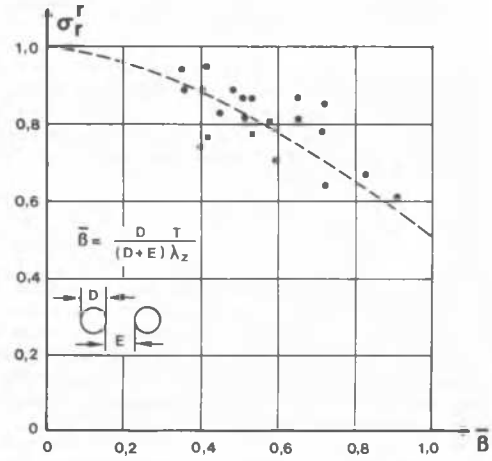

Fig. 13: Ampl. reduction factor vs normalized shielded area

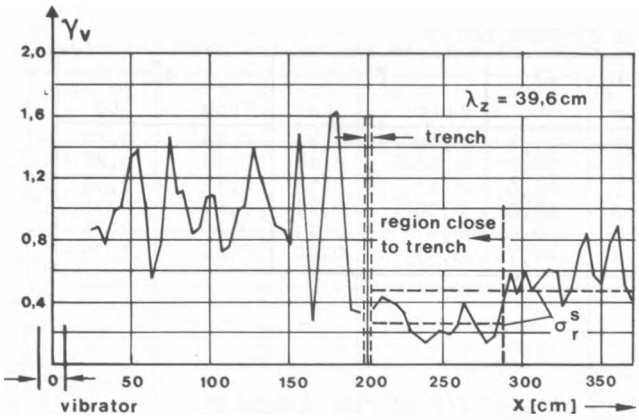

Fig. 14: Normalized amplitude, open trench

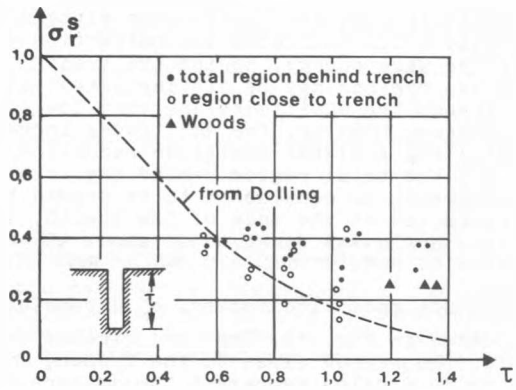

Fig. 15: Ampl. reduction factor vs trench depth

trench being totally reflected. The part below the trench, however, is transmitted beneath the trench and transformed to a new Rayleigh wave, having a smaller amplitude corresponding to the smaller content of energy.

This theory is in good agreement with the experimental results if only the region close to the trench is considered. If, however, the total region behind the trench is involved the isolation effectiveness is overestimated.

CONCLUSION

Experimental investigations in model scale have been performed on the screening effect of different vibration isolation measures in the ground. The average amplitude reduction of a steady-state, harmonic wave field caused by the isolation measures is used to describe their screening effectiveness.

At solid obstacles designed to represent concrete core walls at full scale the results have been found to agree very well with those of FE-calculations performed on this problem. They show the screening effect of these barriers not to be a function of the cross sectional shape but only of the normalized cross sectional area.

At rows of bore holes stabilized by plastic tubes an increase of the isolation effect with increasing normalized shielded area was found.

The screening effect of open trenches is increased with the normalized depth. The results obtained in this study are in good agreement with those of other investigations.

ACKNOWLEDGEMENT

The writer is grateful for the support of this investigation by the german Minister of Constructions and City Planning.The suggestions and encouragement of G.Gudehus and the aid in performing the tests of P.Sanio are gratefully acknowledged.

REFERENCES

Dolling, H.J. (1970). Abschirmung von Erschütterungen durch Bodenschlitze. Die Bautechnik, Heft 5/6

Gudehus, G., W.Haupt (1978). Abschirmung von Untergrunderschütterungen an Bauwerken. Research report to the Minister of Construction and City-Planning, Az. BI5 - 80 01 75-40

Haupt, W. (1978 a). Verhalten von Oberflächenwellen im inhomogenen Halbraum mit besonderer Berücksichtigung der Wellenabschirmung. Report of the Institute of Soil and Rock Mech., Univ. of Karlsruhe, No. 74

Haupt, W. (1978 b). Surface Waves in Non-Homogeneous Half-Space. Proc. Dyn. Meth. in Soil and Rock Mech. (DMSR 77), Vol 1, A.A. Balkema Publ., Rotterdam

Haupt, W. (1978 c). Numerical Methods for the Computation of Steady-State Harmonic Wave Fields. Proc. Dyn. Meth. in Soil and Rock Mech. (DMSR 77), Vol 1, A.A. Balkema Publ., Rotterdam

Miller, G.F., H.Pursey (1954). The field and radiation impedance of mechanical radiators on the free surface of a semi-infinite, isotropic solid. Royal Soc., Proc., Serie A, Vol. 233

Segol. G., P.C.Y.Lee, J.F. Abel (1978). Amplitude Reduction of Surface waves by Trenches. ASCE Proc., No EM3, June

Woods, R.D. (1968). Screening of Surface Waves in Soils. ASCE Proc., No SM4, July

Woods, R.D., N.E. Barnett, R. Sagesser (1974). Holography - A New Tool for Soil Dynamics. ASCE Proc., No GT11, Nov.